Brain Struct Funct
DOI 10.1007/s00429-014-0779-8

ORIGINAL ARTICLE

Dietary magnesium restriction reduces amygdala–hypothalamic GluN1 receptor complex levels in mice

Maryam Ghafari · Nigel Whittle · András G. Miklósi · Caroline Kotlowsky · Claudia Schmuckermair · Johannes Berger · Keiryn L. Bennett · Nicolas Singewald · Gert Lubec

Received: 26 July 2013 / Accepted: 11 April 2014

Abstract Reduced daily intake of magnesium (Mg^{2+}) is suggested to contribute to depression. Indeed, preclinical studies show dietary magnesium restriction (MgR) elicits enhanced depression-like behaviour establishing a causal relationship. Amongst other mechanisms, Mg^{2+} gates the activity of *N*-methyl-D-asparte (NMDA) receptors; however, it is not known whether reduced dietary Mg^{2+} intake can indeed affect brain NMDA receptor complexes. Thus, the aim of the current study was to reveal whether MgR induces changes in brain NMDA receptor subunit composition that would indicate altered NMDA receptor regulation. The results revealed that enhanced depression-like behaviour elicited by MgR was associated with reduced amygdala–hypothalamic protein levels of GluN1-containing NMDA complexes. No change in GluN1 mRNA levels was observed indicating posttranslational changes were induced by dietary Mg^{2+} restriction. To reveal possible protein interaction partners, GluN1 immunoprecipitation and proximity ligation assays were carried out revealing the expected GluN1 subunit association with GluN2A, GluN2B, but also novel interactions with GluA1, GluA2 in addition to known downstream signalling proteins. Chronic paroxetine treatment in MgR mice normalized enhanced depression-like behaviour, but did not alter protein levels of GluN1-containing NMDA receptors, indicating targets downstream of the NMDA receptor. Collectively, present data demonstrate that dietary MgR alters brain levels of GluN1-containing NMDA receptor complexes, containing GluN2A, GluN2B, AMPA receptors GluA1, GluA2 and several protein kinases. These data indicate that the modulation of dietary Mg^{2+} intake may alter the function and signalling of this receptor complex indicating its involvement in the enhanced depression-like behaviour elicited by MgR.

Keywords NMDA · Receptor complexes · Dietary magnesium restriction · Depression · Forced swim test · Amygdala · Hypothalamus

M. Ghafari, N. Whittle contributed equally to this work.

Electronic supplementary material The online version of this article (doi:10.1007/s00429-014-0779-8) contains supplementary material, which is available to authorized users.

M. Ghafari · A. G. Miklósi · C. Kotlowsky · G. Lubec (✉)
Department of Pediatrics, Medical University of Vienna, Währinger Gürtel 18, 1090 Vienna, Austria
e-mail: gert.lubec@meduniwien.ac.at

N. Whittle · C. Schmuckermair · N. Singewald
Department of Pharmacology and Toxicology and Center for Molecular Biosciences, University of Innsbruck, Peter-Mayr Straße 1/1 Stock, 6020 Innsbruck, Austria

J. Berger
Department of Pathobiology of the Nervous System, Center for Brain Research, Medical University of Vienna, Spitalgasse 4, 1090 Vienna, Austria

K. L. Bennett
CeMM Research Center for Molecular Medicine of the Austrian Academy of Sciences, Lazarettgasse 14, AKH Building BT 25.3, 1090 Vienna, Austria

Introduction

Magnesium (Mg^{2+}) is an essential ion and has many diverse functions within the central nervous system including voltage-dependent blocking of *N*-methyl-D-aspartate (NMDA) receptors (Haddad 2005) and is serving as cofactor in over 300 enzymes including tyrosine and tryptophan hydroxylases (Kantak 1988) and enzymes

Published online: 08 May 2014

ubiquitous in energy metabolism (Haddad 2005), glycolysis and the tricarboxylic acid cycle (Cowan 2002; Garfinkel and Garfinkel 1985). Mg^{2+} therefore has a profound influence on many cellular processes including DNA and protein synthesis, intracellular signal transduction, cell growth and differentiation. In the central nervous system, Mg^{2+} plays an important role in neurotransmission: it has been reported that synaptic vesicle recycling depends upon presynaptic concentrations of Mg^{2+} (Koenig and Ikeda 1996) and Mg^{2+} has been shown to modulate both, glutamatergic (via a voltage-dependent block of NMDA receptors; (Haddad 2005) and GABAergic neurotransmission, and to affect numerous transduction pathways, including that of protein kinase C (Murck 2002).

Within NMDA receptors Mg^{2+} is a "gating" ion as it blocks the NMDA receptor ion channel when neurons are in a resting state and Mg^{2+} is removed from the channel during states of depolarization (Cooper et al. 1996).

In Mg^{2+} restriction, it is probable that NMDA receptors allow more Ca^{2+} passing through the receptor channel by the lack of Mg^{2+} blockade within the ion channel. This condition would likely yield neurons containing hypersensitive NMDA receptors and may lead to noisy glutamatergic synapses that would interfere with efficient synaptic processing. In support of this hypersensitivity theory, it was shown that Mg^{2+} deficient mice have a lower threshold for NMDA-induced seizures (Bardgett et al. 2005). Although this hypersensitivity might be expected to produce excitotoxicity, cursory inspections of limbic system brain regions in Mg^{2+}-deficient mice have not revealed overt neuropathology (Saatman et al. 2001).

In humans, Mg deficiency is well-documented to be involved in a series of neuropsychiatric disorders (Eby and Eby 2006). Further strengthening this are the preclinical findings demonstrating that Mg^{2+}-restricted (MgR) diets elicit enhanced depression-like behavior (Singewald et al. 2004; Spasov et al. 2008; Muroyama et al. 2009; Whittle et al. 2011). Importantly, enhanced depression-like behaviour can be reversed following clinically relevant antidepressant, anxiolytic and *Hypericum* extract LI60 treatments (Singewald et al. 2004; Whittle et al. 2011; Sartori et al. 2012).

As stated above, a link between Mg and NMDA receptor-mediated signalling being associated with major depression has been proposed (Murck 2013; Sowa-Kucma et al. 2013) and this formed the rationale to carry out the current investigation. The aim of the study was to determine potential alterations in the subunit composition of NMDAR receptor containing complexes (GluN1, GluN2A, GluN2B) in amygdala/hypothalamus of MgR mice in comparison to control-fed mice and MgR mice chronically co-treated with paroxetine. In addition, 5-hydroxytryptamine receptor 1A (5-HT_{1A}) and dopamine D1 levels were determined in the same experimental groups.

Materials and methods

Animals

Animals were male 2 month old C57Bl/6N (B6) mice (obtained from Charles River, Germany) which were housed (4–5 per cage) in a temperature- (22 ± 2 °C) and humidity-(50–60 %) controlled vivarium under a 12 h light/dark cycle (lights on at 7:00 A.M.). All experimental procedures were approved by the Austrian Animal Experimentation Ethics Board (Bundesministerium für Wissenschaft und Verkehr, Kommission für Tierversuchsangelegenheiten).

Control and magnesium-restricted diets

10 B6 mice were fed commercially prepared food pellets (ssniff Spezialdiäten, Soest, Germany) containing low Mg [MgR; 100 mg/kg food which provides about 20 % of daily requirements (Kantak 1988)] or standard food pellets containing normal quantities of Mg [$n = 10$; Ctl; 0.2 % Mg, which is four times more than the minimum Mg requirement of 500 mg/kg of food (Kantak 1988)] for 3 weeks before quantification of depression- or anxiety-like behaviours and through to the completion of the experiment as previously described (Singewald et al. 2004). No seizures or other adverse reactions were observed in animals on these diets.

Effects of chronic paroxetine administration

Paroxetine (Sigma-Aldrich, St. Louis, MO, USA) was administered to a group of 10 Mg-restricted B6 mice (MgR-PAR) via drinking water at a daily dose of 5 mg/kg body weight (calculation was based on drinking water consumption) as previously described for 3 weeks before quantification of depression-like behaviour (Whittle et al. 2011).

Quantification of depression-like behaviour

Mice were subjected to the forced swim test as previously described (Singewald et al. 2004). Mice were individually placed in an open cylinder (diameter 12 cm, height 20 cm) containing 16-cm deep fresh tap water maintained at 23 °C. Their activity was videotaped over a period of 6 min. The illumination was set at 100 lux. The total time of immobility was measured during the last 4 min of testing by an observer blinded to the treatments. Mice were considered immobile when floating passively in the water, performing only those movements required for keeping their heads above the water level.

Biochemical analyses

Tissue extraction, glucose gradient centrifugation, blue native-polyacrylamide gel electrophoresis and Western blotting

On the fourth day following the forced swim test, mice were killed by carbon dioxide inhalation in a chamber in accordance with the established welfare guidelines (Hackbarth et al. 2000). Brains were rapidly removed from the skull and a tissue block containing whole amygdala and hypothalamus (−0.46 to −3.40 mm Bregma) was taken on a chilled metal plate and subsequently stored at −80 °C; the freezing chain was never interrupted. Amygdala–hypothalamic brain blocks were then subjected to either immunoblotting studies (n = 8–10/group) or rt-PCR (n = 10/group) analysis.

Sample preparation for determination of receptor complexes

Individual samples were homogenized in ice-cold homogenization buffer [10 mM HEPES, pH 7.5, 300 mM sucrose, one complete protease inhibitor tablet (Roche Molecular Biochemicals, Mannheim, Germany) per 50 mL] by Ultra-Turrax® (IKA, Staufen, Germany). The homogenate was centrifuged for 10 min at 1,000×g and the pellet was discarded. The supernatant was centrifuged at 50,000×g for 30 min in an ultracentrifuge (Beckman Coulter Optima® L-90K). Subsequently, the pellet was homogenized in 5 mL washing buffer (homogenization buffer without sucrose), kept on ice for 30 min and centrifuged at 50,000×g for 30 min (Ghafari et al. 2012a).

Sucrose gradient ultracentrifugation

The plasma membrane purification procedures from the pellet were carried out as described previously, with slight modifications (Chen et al. 2006; Kang et al. 2008). Sucrose density gradient centrifugation solutions of 700 µL each of 69, 54, 45, 41, and 37 % (w/v) were formed. Membrane pellets in 500 µL were resuspended in homogenization buffer, layered on top of the tubes that were filled with homogenization buffer. Samples were ultracentrifuged at 4 °C at 70,000×g for 3 h. After centrifugation, the 41 % fraction from the sucrose interface was collected, diluted 10 times with homogenization buffer, and then ultracentrifuged at 4 °C at 100,000×g for 30 min. After discarding the supernatant, the pellet was stored at −80 °C until use.

Blue native-polyacrylamide gel electrophoresis (BN-PAGE)

Membrane pellets from the 41 % sucrose gradient ultracentrifugation fraction were solubilized in extraction buffer [1.5 M 6-aminocaproic acid, 300 mM Bis–Tris, pH 7.0] and 10 % n-dodecyl b-D-maltoside with vortexing every 10 min for 1 h. Following solubilization, samples were cleared by centrifugation at 20,000×g for 60 min at 4 °C. The protein content was estimated using the BCA protein assay kit (Pierce, Rockford, IL, USA).

20 µg of membrane protein for 5-HT_{1A}, 80 µg for GluN1 and D1, 50 µg for GluN2A and GluN2B were applied on to gels. 16 µL BN-PAGE loading buffer [5 % (w/v) Coomassie G250 in 750 mM 6-aminocaproic acid] were mixed with 100 µL of the membrane protein preparation and loaded on to the gel. BN-PAGE was performed in a PROTEAN II xi Cell (BioRad, Germany) using 4 % stacking and 5–18 % separating gel.

The BN-PAGE gel buffer contained 500 mM 6-aminocaproic acid, 50 mM Bis–Tris, pH 7.0; the cathode buffer 50 mM Tricine, 15 mM Bis–Tris, 0.05 % (w/v) Coomassie G250, pH 7.0; and the anode buffer 50 mM Bis–Tris, pH 7.0. The voltage was set to 50 V for 1 h, 75 V for 6 h, and was increased sequentially to 400 V (maximum current 15 mA/gel, maximum voltage 500 V) until the dye front reached the bottom of the gel (Ghafari et al. 2012a). Native high-molecular mass markers were obtained from Invitrogen (Carlsbad, CA, USA).

Western blotting

Membrane proteins were transferred from BN-PAGE to PVDF membranes. After blocking of membranes for 1 h with 10 % nonfat dry milk in 0.1 % TBST (100 mM Tris–HCL, 150 mM NaCl, pH 7.5, 0.1 % Tween 20), membranes were incubated with diluted primary antibodies rabbit anti-mouse NMDA receptor 1 antibody (1:5000, Abcam, Cambridge, UK), rabbit anti-mouse NMDA receptor 2A antibody (1:10000, Abcam, Cambridge, UK), rabbit anti-mouse NMDA receptor 2B antibody (1:500, Abcam, Cambridge, UK), rabbit antimouse anti-5-hydroxytryptamine receptor 1A antibody (1:20000, Genscript, Piscataway, NJ, USA), rabbit antimouse dopamine 1 receptor antibody (1:5000, Abcam, Cambridge, UK) and detected with horseradish peroxidase-conjugated antirabbit IgG (Abcam, Cambridge, UK). Membranes were developed with the ECL Plus Western Blotting Detection System (GE Healthcare, Buckinghamshire, UK). Arbitrary optical densities of immunoreactive bands were measured by the Image J software program (http://www.rsb.info.nih.gov/ij/).

Immunoprecipitation of GluN1 from mouse amygdala and hypothalamus

Pooled total membrane fractions from amygdala and hypothalamus of three mice were suspended in lysis buffer

containing 1 % Triton ×100, 150 mM NaCl, 1 mM EDTA, 50 mM Tris–HCl (pH 8.0), 10 mM NaF, 10 mM Na_3VO_4 and protease inhibitor cocktail (Roche, Mannheim, Germany) on a rotation shaker for 1 h at 4 °C. After centrifugation at 15,300×*g*, at 4 °C for 10 min, the supernatant was incubated with affinity purified goat antibody against GluN1 (glutamate (NMDA) receptor zeta 1; Santa Cruz, Santa Cruz, CA) and subsequently incubated with protein G agarose beads (GE Healthcare, Uppsala, Sweden) for 4 h at 4 °C with gentle rotation. After five times of washing with the same lysis buffer, proteins bound were denatured with sample buffer containing 125 mM Tris (pH 6.8), 4 % SDS, 20 % glycerol, 10 % beta-mercaptoethanol, 0.02 % bromophenol blue at 95 °C for 3 min (Ghafari et al. 2012b).

Samples were loaded on to 10 % SDS–polyacrylamide gels, electrophoresed, and subsequently transferred to PVDF membranes (Pall, Ann Harbor, MI). After blocking of membranes for 1 h with 5 % nonfat dry milk in 0.1 % TBST (100 mM Tris–HCL, 150 mM NaCl, pH 7.5, 0.1 % Tween 20), membranes were incubated with diluted goat primary antibodies against GluN1 (glutamate receptor zeta 1 antibody; 1:5000, Santa Cruz, Santa Cruz, CA), and detected with horseradish peroxidase-conjugated antigoat IgG (1:5,000, Abcam, Cambridge, UK). Membranes were developed with the ECL Plus Western Blotting Detection System (GE Healthcare, Uppsala, Sweden).

In-gel digestion of proteins and peptides

The sample was run on SDS-PAGE and spots picked from the SDS gel were put into a 1.5 mL tube. Gel pieces were washed with 50 mM ammonium bicarbonate and then two times with washing buffer (50 % 100 mM ammonium bicarbonate/50 % acetonitrile) for 30 min each with vortexing. An aliquot of 100 µL of 100 % acetonitrile was added to the tube to cover the gel pieces completely and the mixture was incubated for 10 min. Gel pieces were dried completely using a SpeedVac concentrator. Reduction in cysteine residues was carried out with a 10 mM dithiothreitol (DTT) solution in 100 mM ammonium bicarbonate pH 8.6 for 60 min at 56 °C. After discarding the DTT solution, the same volume of a 55 mM iodoacetamide (IAA) solution in 100 mM ammonium bicarbonate buffer pH 8.6 was added and incubated in darkness for 45 min at 25 °C to achieve alkylation of cysteine residues. The IAA solution was replaced by washing buffer (50 % 100 mM ammonium bicarbonate/50 % acetonitrile) and washed twice for 15 min each with vortexing. Gel pieces were washed and dried in 100 % acetonitrile followed by dryness in SpeedVac. Dried gel pieces were reswollen with 12.5 ng/µL trypsin (Promega, Germany) solution reconstituted with 25 mM ammonium bicarbonate or 12.5 ng/µL chymotrypsin (Roche Diagnostics, Mannheim, Germany) solution buffered in 25 mM ammonium bicarbonate. Gel pieces were incubated for 16 h (overnight) at 37 (trypsin) or 25 °C (chymotrypsin). The supernatant was transferred to new 0.5 mL tubes, and peptides were extracted with 50 µL of 0.5 % formic acid/20 % acetonitrile for 20 min in a sonication bath. This step was repeated two times. Samples in extraction buffer were pooled in 0.5 mL tubes and evaporated in a SpeedVac concentrator. The volume was reduced to approximately 20 µL and then 20 µL HPLC grade water (Sigma, St. Louis, MO) and used for analysis on a LTQ Orbitrp Velos mass spectrometer (Ghafari et al. 2012b).

Mass spectrometry

Mass spectrometry was performed on a hybrid LTQ Orbitrap Velos mass spectrometer (ThermoFisher Scientific, Waltham, MA, USA) using Xcalibur version 2.1.0 SP1.1160 coupled to an Agilent 1200 HPLC nanoflow system (dual pump with one precolumn and one analytical column) (Agilent Biotechnologies, Palo Alto, CA, USA) via a nanoelectrospray ion source using liquid junction (Proxeon, Odense, Denmark). Solvents for HPLC separation of peptides were as follows: solvent A consisted of 0.4 % formic acid (FA) in water and solvent B consisted of 0.4 % FA in 70 % methanol and 20 % isopropanol. From a thermostated microautosampler, 8 µL of the tryptic peptide mixture was automatically loaded on to a trap column (Zorbax 300SB-C18 5 µm, 5 × 0.3 mm, Agilent Biotechnologies, Palo Alto, CA, USA) with a binary pump at a flow rate of 45 µL/min. 0.1 % trifluoroacetic acid (TFA) was used for loading and washing the precolumn. After washing, the peptides were eluted by back-flushing on to a 16-cm fused silica analytical column with an inner diameter of 50 µm packed with C18-reversed phase material (ReproSil-Pur 120 C18-AQ, 3 µm, Dr. Maisch GmbH, Ammerbuch-Entringen, Germany). The peptides were eluted from the analytical column with a 27 min gradient ranging from 3 to 30 % solvent B, followed by a 25 min gradient from 30 to 70 % solvent B and, finally, a 7 min gradient from 70 to 100 % solvent B at a constant flow rate of 100 nL/min (Bennett et al. 2011). The analyses were performed in a data-dependent acquisition mode and dynamic exclusion for selected ions was 60 s. A top 15 collision-induced dissociation (CID) method was used, and a single lock mass at *m/z* 445.120024 $(Si(CH_3)_2O)_6$) (Olsen et al. 2005) was employed. Maximal ion accumulation time allowed in CID mode was 50 ms for MS^n in the LTQ and 500 ms in the C-trap. Automatic gain control was used to prevent overfilling of the ion traps and was set to 5,000 in MS^n mode for the LTQ and 10^6 ions for a full FTMS scan. Intact peptides were detected in the Orbitrap Velos at

60,000 resolution at *m/z* 400. All samples were analyzed as technical duplicates. The acquired raw MS data files were processed with msconvert (ProteoWizard Library v2.1.2708) and converted into MASCOT generic format (mgf) files.

MASCOT searches were done by using the MASCOT 2.2.06 (Matrix Science, London, UK) against latest UniProtKB database for protein identification. Searching parameters were set as follows: enzyme selected as trypsin or chymotrypsin with three maximum missing cleavage sites, species taxonomy: limited to mice, a mass tolerance of 10 ppm for peptide tolerance, 0.6 Da for MS/MS tolerance, ions score cutoff lower than 15, fixed modification of carbamidomethyl (C) and variable modification of oxidation (M), and phosphorylation (S, T, Y). Positive protein identifications were based on a significant MOWSE score. After protein identification, an error-tolerant search was done to detect unspecific cleavage and unassigned modifications. Protein identification and modification information returned were manually inspected and filtered to obtain confirmed protein identification and modification lists The values lower than 0.1 (or higher than score 27) were selected for high significance (Ghafari et al. 2012b).

Real-time PCR

Total RNA was isolated from frozen amygdala/hypothalamus tissues using TRIzol Reagent (Invitrogen, Carlsbad, CA) and a Polytron PT3100 homogenizer (Kinematica, CA) followed by a second step of purification using RNeasy mini kit (Qiagen, Bothell, WA) including a DNase I digestion step (RNase-free DNase set Qiagen). For each assay, 4 ng cDNA (generated by QuantiTect Reverse Transcription Kit, Qiagen) were analyzed using the CFX96 real-time PCR detection system (Bio-Rad, Hercules, CA). Mouse GluN1 expression was quantified using the primers Oli. 1888 nt 1799 5′-CAGGAGCGGGTAAACAACAGC-3′ (forward) and Oli. 1889 nt 2001 5′-AATGAGTCCAGTGTGCTC CG-3′ (reverse) (Acc. No. NM_001177656.1) with SsoFast EvaGreen (Bio-Rad,Germany). As a control, glyceraldehyde-3-phospate dehydrogenase (Gapdh) mRNA levels were quantified using the primers Oli. 470 nt529, 5́-AGG TCATCCATGACAACTTT-3́ (forward), Oli. 471 nt605, 5́-AGTCTTCTGGGTGGCAGT-3́ (reverse), nt566, 5́-FAM CATGACCACAGTCCATGCCA -DABCYL-3́ (TaqMan probe) (Acc. No. NM_008084.2). Standard curves were generated by serial dilution of plasmids containing GluN1 (P1645; BioCat IMAGE ID 4507986) or Gapdh (P283; Weinhofer et al. 2002) cDNA. The thermocycler was programmed: 95 °C for 30 s followed by 49 cycles at 95 °C for 5 s and 56 °C for 10 s for Gapdh and 95 °C for 30 s followed by 49 cycles at 95 °C for 5 s and 60 °C for 5 s for GluN1. At the end of the GluN1 EvaGreen-detection, a melt curve was performed for each well to ensure the absence of unspecific PCR products (Weinhofer et al. 2002).

Proximity ligation assay

Animal perfusion and brain preparation

Three C57Bl/6 N mice were anesthetized with 0.3 ml/kg intraperitoneal injection of sodium penthorbital (Release, 300 mg/ml, Wirtschaftsgenossenschaft deutscher Tierärzte eG, Garbsen, Germany) and perfused intracardially with ice-cold PBS (0.1 M phosphate buffered saline, pH 7.2) containing 0.2 % heparin followed by 4 % paraformaldehyde (PFA) at a pH of 7.4 in PBS. Brain samples were post-fixed in 4 % PFA for 24 h at 4 °C then transferred into a 30 % sucrose solution (PBS) for 48 h. Brains were frozen at −20 °C with Tissue-Tek media (OCT compound, Sakura Finetek Europe, The Netherlands) and sectioned at 30 µm with a cryostat (Leica CM 3050S, Wetzlar, Germany). Sections were stored in PBS with 0.01 % of sodium azide until further processing.

"In situ" proximity ligation assay (PLA)

The PLA was performed according to the protocol given by the manufacturer (O-LINK Bioscience, Uppsala, Sweden) with slight modifications. Free floating brain slices were blocked for 30 min at room temperature using blocking buffer supplied with the PLA kit. After blocking, brain slices were incubated with diluted primary antibodies: rabbit monoclonal antibody against NMDA receptor 1(GluN1; 1:100, Abcam, Cambridge, UK), mouse monoclonal antibody against NMDA receptor 2B (GluN2B; 1:100, Abcam, Cambridge, UK) for detection of the GluN1-GluN2B complex and mouse monoclonal antibody against NMDA receptor 1 (1:100, Abcam, Cambridge, UK), rabbit polyclonal antibody against the NMDA receptor 2A (GluN2A; 1:100, Abcam, Cambridge, UK) for detection of the GluN1–GluN2A complex for 48 h at 4 °C on a rocking platform Following incubation with primary antibodies slices were washed with washing buffer A (O-LINK Bioscience, Uppsala, Sweden) and subsequently incubated with rabbit PLUS and mouse MINUS probes (1:40, O-LINK Bioscience, Uppsala, Sweden) for 2 h at 37 °C with gentle orbital shaking. Ligation was performed according to the manufacturer's protocol with the exception of a 45 min incubation time instead of 30 min as recommended. DNA polymerase was diluted 1:40 and incubated for 120 min at 37 °C. The other amplification steps were following the instructions in the manual as given above. After amplification, slices were washed with 1× then 0.01× washing buffer B prepared according to the recipe supplied in the kit manual. Finally, brain slices were

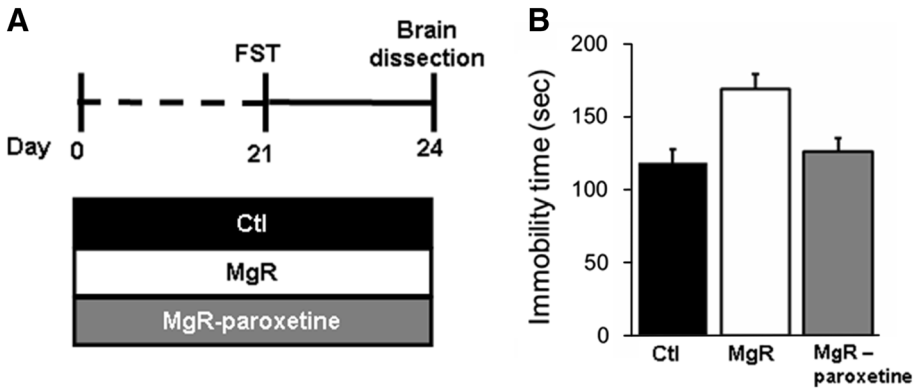

Fig. 1 **a** Diagram of treatments. Controls were fed the standard rodent diet, Mg restriction and/or paroxetine treatment was carried out for 24 days. **b** The forced swim test was performed on day 21.MgR lead to increased immobility that was reversed by paroxetine treatment. *Bars* in Figs. 1, 2, 3 and 4 represent standard deviations

transferred to glass slides, mounted with Duolink in situ Mounting Medium with DAPI (O-LINK Bioscience, Uppsala, Sweden). Images were acquired with a Zeiss LSM 700 confocal laser scanning microscope (Carl Zeiss GmbH, Jena, Germany) at 20× magnification keeping all acquisition settings even throughout all samples.

Statistical analysis

The results were analyzed by ANOVA. The level of probability was considered significant at $P < 0.05$. Data from Western blotting were handled by ANOVA followed by a *t* test, and data are given as mean ± SD. Correlations between behavioral output measures and receptors complex levels were performed using the Spearman's coefficient test. Statistical analysis for the quantification of RT-PCR results was carried out using the Student's *t* test.

Results

Behavioral studies

After 21 days of the commencement of the diet and/or chronic paroxetine treatments, all experimental groups were subjected to the forced swim test (Fig. 1a). One-way ANOVA revealed that immobility times differed between groups ($F_{(2,23)} = 7.40$, $p < 0.01$). Bonferroni's post hoc testing revealed that MgR displayed a higher immobility time as compared to controls ($p < 0.01$) (Fig. 1b) indicating enhanced depression-like behavior. Chronic paroxetine treatment normalized enhanced depression-like behavior in Mg-restricted mice ($p < 0.05$, MgR-PAR vs MgR) to the level of controls (Fig. 1b).

Receptor complex levels

Using BN-PAGE followed by immunoblotting with specific antibodies against the NMDAR subunit GluN1, a significantly reduced GluN1-containing NMDAR complex

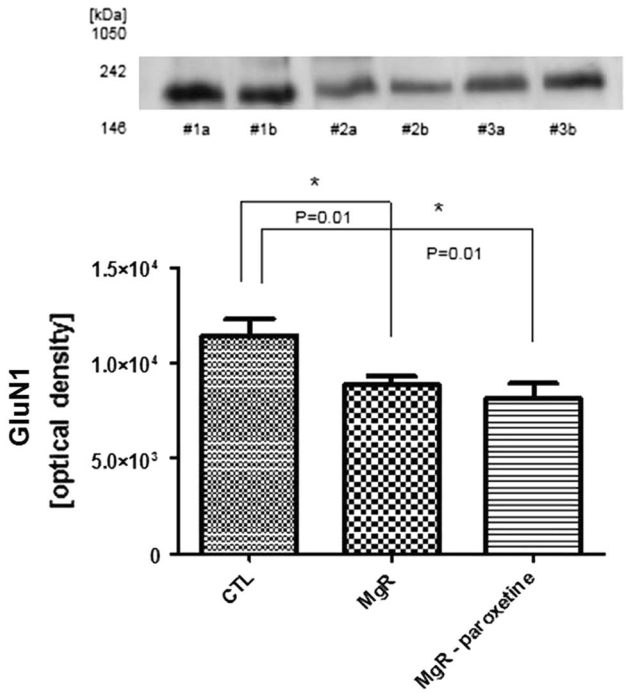

Fig. 2 A single band was observed representing the GluN1-containing complex, which was significantly reduced in Mg restriction and in MgR with paroxetine treatment. Representative images of Western blots 1a,b controls, 2a,b MgR, 3a,b MgR + paroxetine treatment

migrating at the apparent molecular weight between 146 and 242 kDa was observed in the Mg^{2+} restricted group as well as in the Mg^{2+} restricted group with paroxetine treatment as compared to controls (Fig. 2).

Levels for a GluN2A-containing NMDAR complex that was observed between 480 and 720 kDa were comparable between groups (Supplemental Fig. 1). Levels for a GluN2B-containing NMDAR complex migrating between 480 and 720 kDa that may well be the same complex containing GluN2A (Ghafari et al. 2011) were significantly increased in the Mg^{2+} restricted groups, but showed only a trend towards an increase in paroxetine-treated animals (Fig. 3).

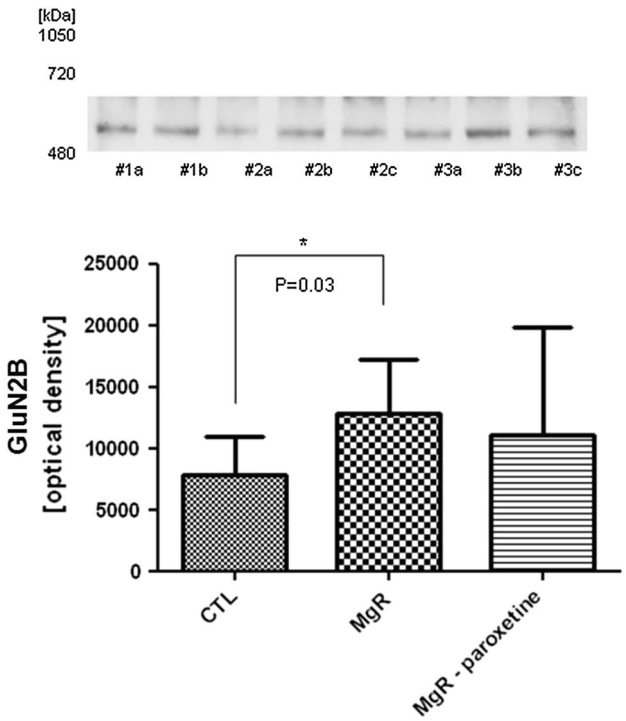

Fig. 3 A single band was representing the GluN2B-containing receptor complex. Complex levels were significantly increased in MgR and showed a trend to increased levels in MgR with paroxetine treatment

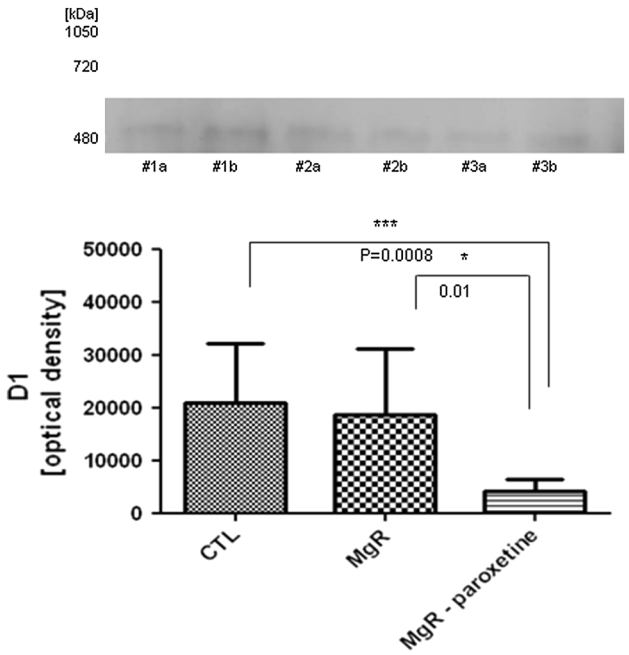

Fig. 4 A single band was representing the D1-receptor complex and this was significantly and remarkably decreased in the paroxetine-treated group and is proposed to be a drug effect

A D1-containing receptor complex was migrating between 480 and 720 kDa although the precision of the technique would not allow to propose that the D1 subunit was a constituent of the GluN2A/GluN2B complex. Levels for the D1-containing receptor complex were comparable between controls and Mg^{2+} restriction; however, levels were significantly decreased in animals with paroxetine treatment when this group was as compared to both, controls and Mg^{2+}-restricted animals, which would be compatible with a drug effect (Fig. 4).

Amygdala/hypothalamic complex levels containing 5-HT_{1A}R and migrating at approximately 480 kDa were comparable between groups (Supplemental Fig. 2).

Correlation analysis between receptor complexes showed a link between levels of the GluN1 and GluN2A-containing receptor complexes ($R = 0.43$, $P = 0.025$; Fig. 5a; Supplemental Table 1). In addition, GluN1- as well as GluN2A-containing complexes were associated with D1-containing receptor complexes (Fig. 5b, c; $R = 0.53$, $P = 0.004$; $R = 0.38$, $P = 0.04$).

There was no significant correlation between any parameter tested in the forced swim test with any of the receptor complexes as shown in Supplemental Table 2.

As shown in Supplemental Fig. 3, there were no significant differences between mRNA levels for GluN1 between samples from controls and Mg^{2+} restricted animals strongly indicating that regulation of the complex formation may be based upon protein stability or assembly.

Composition of the GluN1-containing receptor complex

As shown in Fig. 6a several proteins from immunoprecipitation using an antibody against the GluN1 subunit were revealed on SDS-PAGE. Bands were picked according to the Western blotting pattern to demonstrate position for the GluN1 subunit (Fig. 6b) and from other positions in the gel and mass spectrometry unambiguously identified GluN1, GluN2A, GluN2B, GluA1-4, serine-threonine protein kinase PAK1 and calcium/calmodulin kinase II subunits alpha, delta and beta (Table 1). The peptides and mass spectrometry data used for unambiguous identification of proteins from this complex are shown in the Supplemental Table 3.

As shown in Fig. 7 and Supplementary Fig. 4 proximity ligation assay revealed the complex formation between GluN1, GluN2A, GluN2B, GluA1 and GluA2. The PLA results would show that the receptors would most probably be in a complex due to the proximity of receptor pairs of <30 nm and this assay was already proposed for generation of evidence for complex formation in general and receptor dimerization in particular (Trifilieff et al. 2011; Augusto et al. 2013).

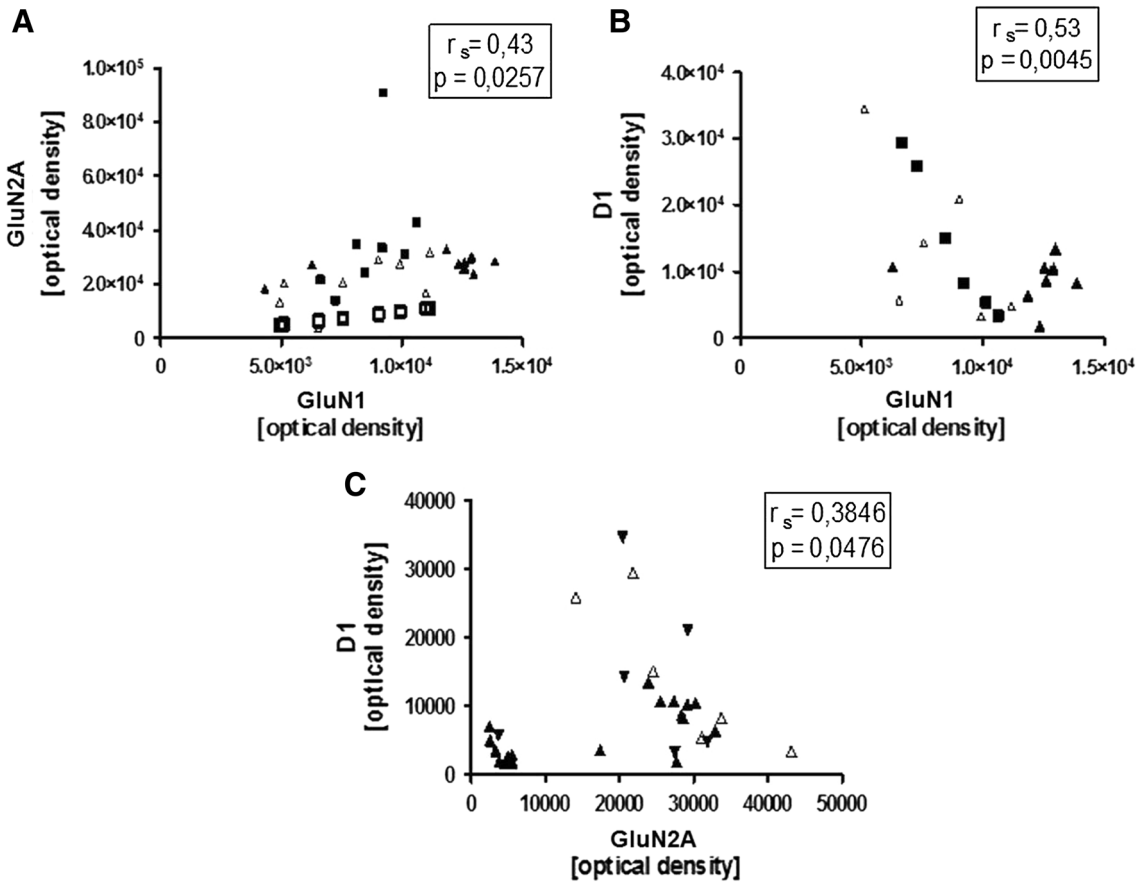

Fig. 5 Significant correlations between the GluN1-containing receptor complex, D1- and GluN2A-containing complexes, as well as between D1- and GluN2A-containing receptor complexes. Correlation coefficients and probabilities of significant correlations are provided showing a link between receptor systems

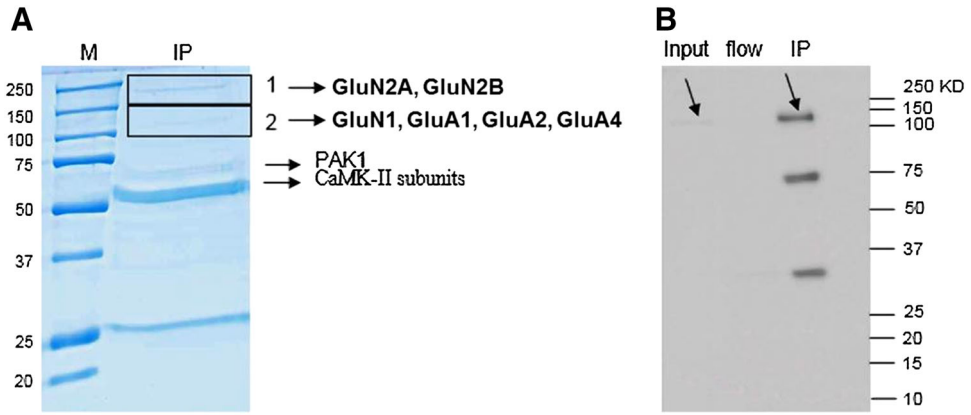

Fig. 6 The SDS gel electrophoretic pattern from the immunoprecipitation from which mass spectrometrical identification of complex constituents were identified (**a**). The immunoblotting pattern of GluN1immunoreactive proteins revealed a single band for GluN1 at the expected molecular weight of 100 kDa. The two bands at the lower apparent molecular weights are representing light and heavy chains of IgG (**b**)

Discussion

The major finding of the current study is the significant reduction in the levels of a GluN1-containing NMDA receptor complex that consisted of GluN2A, 2B, GluA1,2, calcium-calmodulin-dependent kinase II, subunit alpha, beta and delta, as well as serine/threonine protein kinase PAK1. This provides further evidence for the involvement

Table 1 Mass spectrometrical identification of the heteromeric GluN1-containing receptor complex

Accession number	Enzyme	Sequence coverage (%)	Molecular weight (expected) (kDa)	Total amino acids	Total sequence coverage (%)
P35438	Trypsin	46	105.481	938	63.64
GluN1	Chymotrypsin	44			
Q01097	Trypsin	48	165.959	1.482	60.19
GluN2B	Chymotrypsin	15			
P35436	Trypsin	21	165.421	1.464	22.54
GluN2A	Chymotrypsin				
P23819	Trypsin	24	98	883	31.7
GluA2	Chymotrypsin	9			
P23818	Trypsin	11	101	907	15
GluA1	Chymotrypsin	3			
P11798	Trypsin	49	54,115	478	49
CaMK-II subunit alpha					
Q6PHZ2	Trypsin	36	56	499	36
CaMK-II subunit delta					
P28652	Trypsin	48	60	542	48
CaMK-II subunit beta					
088643	Trypsin	11	60	545	11
Serine/threonine protein kinase PAK 1					

Accession numbers in UNIPROT/Swiss-Prot-Expasy, proteases used for in-gel digestion, sequence coverage, expected molecular weight, total amino acids and total sequence coverage are shown

of NMDA receptors in dietary Mg^{2+} restricted-induced depression-like behavior. Involvement of the NMDA receptor system in depression-related behavior has been previously proposed as NMDA receptor antagonists (Layer et al. 1995; Maj et al. 1992; Przegalinski et al. 1997; Trullas and Skolnick 1990; Dunn et al. 1989; Plaznik et al. 1994) and genetic downregulation of the GluN1 subunit of NMDA receptors (Duncan et al. 2009) reduces depression-like behavior in validated rodent tests.

So far, there is no biochemical evidence for NMDA receptor changes in Mg-induced depression-related behavior at the protein level, neither at the NMDA receptor subunit nor at the NMDA receptor complex level. Our study is the first to reveal that reduced dietary intake of Mg^{2+} can dynamically regulate the subunit composition of NMDA receptors. The GluN1 subunit is required for the assembly of functional NMDA receptors (Zukin and Bennett 1995) and can affect the association of the subunit with signalling and structural molecules, including calcium-calmodulin-dependent kinase II (Leonard et al. 2002). Indeed the present finding revealed that the GluN1 subunit displayed an interaction with calcium-calmodulin-dependent kinase II in MgR, providing first information regarding potential deregulated signalling pathways following reduced dietary intake of Mg^{2+}.

Current data suggest that the reduction in GluN1 following dietary Mg^{2+} restriction is not due to altered transcription as we observed comparable gene expression of GluN1 between MgR and control diet-fed mice. This result suggests that reduced GluN1-containing receptor complexes were either due to different assembly of GluN1 subunits in NMDA receptor complexes or that GluN1 protein levels changed due to reduced protein stability; i.e., degradation. NMDA receptor level changes may also be related to increased GluN2B, which is a crucial regulator of trafficking and assembly of triheteromeric receptor complexes (GluN1/GluN2A/GluN2B; (Tang et al. 2010; Akashi et al. 2009).

A novel finding in the present data was that the AMPA receptors GluA1 and GluA2 were shown to interact with GluN1-containing NMDA receptor complexes. GluA1 and GluA2 are the most abundant expressed subunits in AMPA receptors (Wenthold et al. 1996), and has been demonstrated to be directly phosphorylated by a number of proteins including calcium-calmodulin-dependent kinase II (Barria et al. 1997) to enhance receptor function. AMPA and NMDA receptor are both phosphorylated by calcium-calmodulin-dependent kinase II (Tan et al. 1994; Yakel et al. 1995; Bayer et al. 2001, 2006), but in our assay system we cannot differentiate which of the receptors in the complex is phosphorylated by this protein kinase and this may well be in line with the proposed role of AMPA receptors in the FST (Gould et al. 2008; Wlaz et al. 2011) and in particular, GluA1 (syn.: GluA-R1) knockout mice

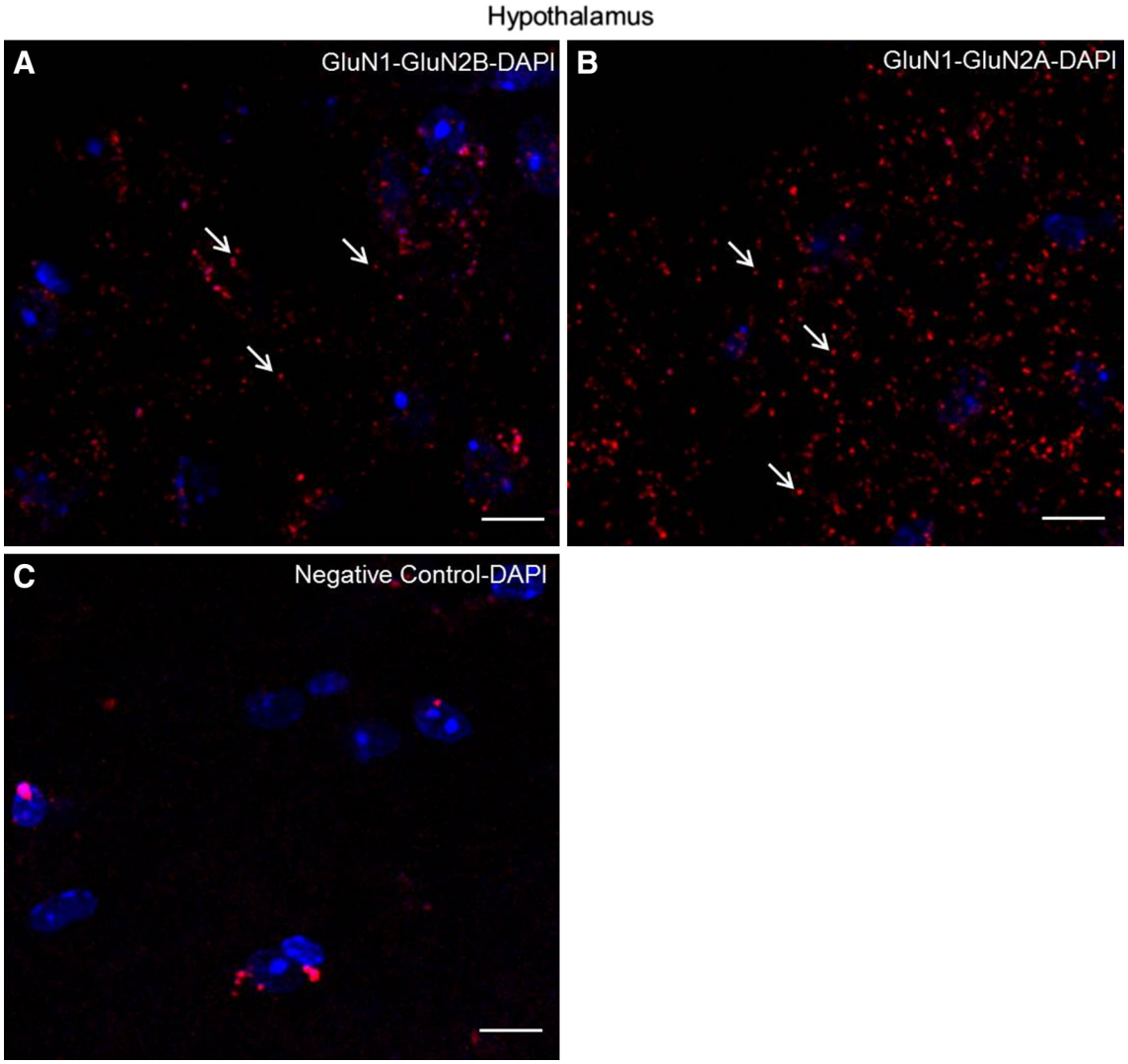

Fig. 7 Detection of GluN1-GluN2B and GluN1–GluN2A receptor complexes by "In Situ" proximity ligation assay (PLA). Representative images showing the GluN1–GluN2B **a** and GluN1–GluN2A **b** receptor complex with DAPI counterstained nuclei in mouse hypothalamus. Each PLA signal represents the interaction of a single GluN1 receptor with a GluN2B, GluN2A receptor, respectively. Negative control with no primary antibody and DAPI counterstaining. **c** The *arrows* indicate examples of PLA signals. Confocal microscope images acquired at 20× magnification. *Scale bar* 10 μm

model the glutamate hypothesis of depression (Chourbaji et al. 2008).

Further characterization of proteins, which interact with the GluN1 subunit revealed several protein kinases; namely, calcium-calmodulin-dependent kinase II (subunits alpha, beta and delta) and serine/threonine protein kinase PAK1. Calcium-calmodulin-dependent kinase II (subunits alpha, beta and delta), is known to translocate to NMDA receptors in an activity-dependent manner (Bayer et al. 2001, 2006; Merrill et al. 2005) and the significance of this finding is probably initiating receptor trafficking, assembly and activation.

The finding that serine/threonine protein kinase PAK1 interacts with the GluN1 subunit of NMDA receptors is a novel and important finding. Protein kinase PAK1 regulates crucial roles in neuronal cell fate, in axonal guidance and neuronal polarization as well as in neuronal migration (Kreis and Barnier 2009) and we show for the first time an association with an NMDA receptor complex. The functional consequence of protein kinase PAK1 phosphorylating NMDA receptors remains to be determined.

In the current study, the GluN2A subunit of NMDA receptors and 5-hydroxytryptamine receptor 1A receptor protein expressions were comparable between MgR and control diet-fed mice indicating that these receptor complexes are not modulated by Mg^{2+}-restriction-induced mechanisms, although it has been shown that the genetic inactivation of GluN2A reveals anxiolytic and

antidepressant-like effects in mice (Boyce-Rustay and Holmes 2006). Moreover, 5-hydroxytryptamine 1A receptors are necessary and sufficient for the normal formation of circuits underlying (innate) anxiety (Richardson-Jones et al. 2011) and 5-hydroxytryptamine receptor 1A knockout mice are presenting with anxiety-related disorder (Ramboz et al. 1998).

Chronic paroxetine treatment normalized the enhanced depression-like behavior in MgR mice. This result is in line with our previous findings and demonstrates the robustness of paroxetine to exert antidepressant-like effects in pro-depressive MgR mice (Whittle et al. 2011). Reversal of depression-related behavior in MgR mice did not normalize reduced levels of the GluN1-containing complex. This may indicate that paroxetine does not exert its' antidepressant effect through direct interaction with NMDA receptors, but rather at downstream targets. Accumulating experimental evidence suggests that potential targets, include inhibition of nitric oxide synthase. Specifically, we have previously shown that paroxetine normalized aberrant nitric oxide synthase/nitric oxide signalling in MgR mice (Whittle et al. 2011) and that paroxetine can reduce nitrite and nitrate levels, which are markers of nitric oxide synthesis, in human serum (Finkel et al. 1996). Moreover, paroxetine can reduce nitric oxide synthase activity in ex vivo hamster brain cytosols (Finkel et al. 1996) further suggesting that paroxetine can reduce downstream signalling of NMDA receptor-mediated activity in mice.

A specific reduction in dopamine D1 receptors was observed in MgR mice chronically treated with paroxetine, indicating an unambiguous drug effect. Moreover, there was a significant correlation between the GluN1-containing receptor complex and a D1-containing receptor complex that may show the interaction between the two receptor complexes. Chronic fluoxetine administration was proposed to upregulate D1-like receptors but this finding was obtained in terms of D1-ligand-binding to the receptor in the hippocampus and is therefore not in conflict with our results of paroxetine-induced decreased D1-receptor containing complexes (Kobayashi et al. 2012).

Conclusion

Taken together, current data reveal that reduction in the dietary intake of Mg^{2+}, which leads to enhanced depression-like behavior, was associated with a reduction in amygdala–hypothalamic level of the GluN1-containing receptor complex that was not normalized following behaviorally effective treatment with chronic paroxetine. We propose that the reduction in the GluN1-containing receptor complex, containing GluN2A, GluN2B, AMPA receptors GluA1, GluA2 and several protein kinases, is due to altered receptor assembly rather than to decreased GluN1 synthesis as no differences were found between GluN1 mRNA levels. The findings demonstrate that reduction of dietary Mg^{2+} intake alters the composition and signaling of NMDA receptors, which may contribute to the molecular mechanisms leading to enhanced depression-like behavior.

Acknowledgments This work was funded partially by the Austrian Science Fund (FWF): P22931-B18 (to NS and GL), W 1206-B18 SPIN (to NS) and partially sponsored by the Verein zur Durchführung der wissenschaftlichen Forschung auf dem Gebiet der Neonatologie und Kinder intensiv Medizin.

References

Akashi K, Kakizaki T, Kamiya H, Fukaya M, Yamasaki M, Abe M, Natsume R, Watanabe M, Sakimura K (2009) NMDA receptor GluN2B (GluR epsilon 2/NR2B) subunit is crucial for channel function, postsynaptic macromolecular organization, and actin cytoskeleton at hippocampal CA3 synapses. J Neurosci 29(35):10869–10882. doi:10.1523/JNEUROSCI.5531-08.2009

Augusto E, Matos M, Sevigny J, El-Tayeb A, Bynoe MS, Muller CE, Cunha RA, Chen JF (2013) Ecto-5′-nucleotidase (CD73)-mediated formation of adenosine is critical for the striatal adenosine A2A receptor functions. J Neurosci 33(28):11390–11399. doi:10.1523/JNEUROSCI.5817-12.2013

Bardgett ME, Schultheis PJ, McGill DL, Richmond RE, Wagge JR (2005) Magnesium deficiency impairs fear conditioning in mice. Brain Res 1038(1):100–106

Barria A, Derkach V, Soderling T (1997) Identification of the Ca^{2+}/calmodulin-dependent protein kinase II regulatory phosphorylation site in the alpha-amino-3-hydroxyl-5-methyl-4-isoxazole-propionate-type glutamate receptor. J Biol Chem 272(52):32727–32730

Bayer KU, De Koninck P, Leonard AS, Hell JW, Schulman H (2001) Interaction with the NMDA receptor locks CaMKII in an active conformation. Nature 411(6839):801–805. doi:10.1038/35081080

Bayer KU, LeBel E, McDonald GL, O'Leary H, Schulman H, De Koninck P (2006) Transition from reversible to persistent binding of CaMKII to postsynaptic sites and NR2B. J Neurosci 26(4):1164–1174. doi:10.1523/JNEUROSCI.3116-05.2006

Bennett KL, Funk M, Tschernutter M, Breitwieser FP, Planyavsky M, Ubaida Mohien C, Muller A, Trajanoski Z, Colinge J, Superti-Furga G, Schmidt-Erfurth U (2011) Proteomic analysis of human cataract aqueous humour: comparison of one-dimensional gel LCMS with two-dimensional LCMS of unlabelled and iTRAQ(R)-labelled specimens. J Proteomics 74(2):151–166

Boyce-Rustay JM, Holmes A (2006) Genetic inactivation of the NMDA receptor NR2A subunit has anxiolytic- and antidepressant-like effects in mice. Neuropsychopharmacology 31(11):2405–2414. doi:10.1038/sj.npp.1301039

Chen P, Li X, Sun Y, Liu Z, Cao R, He Q, Wang M, Xiong J, Xie J, Wang X, Liang S (2006) Proteomic analysis of rat hippocampal plasma membrane: characterization of potential neuronal-specific plasma membrane proteins. J Neurochem 98(4):1126–1140

Chourbaji S, Vogt MA, Fumagalli F, Sohr R, Frasca A, Brandwein C, Hortnagl H, Riva MA, Sprengel R, Gass P (2008) AMPA receptor subunit 1 (GluR-A) knockout mice model the glutamate hypothesis of depression. FASEB J 22(9):3129–3134. doi:10.1096/fj.08-106450

Cooper JR, Bloom FE, Roth RH (1996) The biochemical basis of neuropharmacology. Oxford, New York, pp 518

Cowan JA (2002) Structural and catalytic chemistry of magnesium-dependent enzymes. Biometals 15(3):225–235

Duncan GE, Inada K, Farrington JS, Koller BH, Moy SS (2009) Neural activation deficits in a mouse genetic model of NMDA receptor hypofunction in tests of social aggression and swim stress. Brain Res 1265:186–195. doi:10.1016/j.brainres.2009.02.002

Dunn RW, Corbett R, Fielding S (1989) Effects of 5-HT1A receptor agonists and NMDA receptor antagonists in the social interaction test and the elevated plus maze. Eur J Pharmacol 169(1):1–10. pii:0014-2999(89)90811-X

Eby GA, Eby KL (2006) Rapid recovery from major depression using magnesium treatment. Med Hypotheses 67(2):362–370

Finkel MS, Laghrissi-Thode F, Pollock BG, Rong J (1996) Paroxetine is a novel nitric oxide synthase inhibitor. Psychopharmacol Bull 32(4):653–658

Garfinkel L, Garfinkel D (1985) Magnesium regulation of the glycolytic pathway and the enzymes involved. Magnesium 4(2–3):60–72

Ghafari M, Patil SS, Hoger H, Pollak A, Lubec G (2011) NMDA-complexes linked to spatial memory performance in the Barnes maze in CD1 mice. Behav Brain Res 221(1):142–148

Ghafari M, Falsafi SK, Hoeger H, Lubec G (2012a) Hippocampal levels of GluR1 and GluR2 complexes are modulated by training in the Multiple T-maze in C57BL/6J mice. Brain Struct Funct 217(2):353–362

Ghafari M, Hoger H, Keihan Falsafi S, Russo-Schlaff N, Pollak A, Lubec G (2012b) Mass spectrometrical identification of hippocampal NMDA receptor subunits NR1, NR2A-D and five novel phosphorylation sites on NR2A and NR2B. J Proteome Res 11(3):1891–1896. doi:10.1021/pr201099u

Gould TD, O'Donnell KC, Dow ER, Du J, Chen G, Manji HK (2008) Involvement of AMPA receptors in the antidepressant-like effects of lithium in the mouse tail suspension test and forced swim test. Neuropharmacology 54(3):577–587. doi:10.1016/j.neuropharm.2007.11.002

Hackbarth H, Kuppers N, Bohnet W (2000) Euthanasia of rats with carbon dioxide—animal welfare aspects. Lab Anim 34(1):91–96

Haddad JJ (2005) *N*-methyl-D-aspartate (NMDA) and the regulation of mitogen-activated protein kinase (MAPK) signaling pathways: a revolving neurochemical axis for therapeutic intervention? Prog Neurobiol 77(4):252–282

Kang SU, Fuchs K, Sieghart W, Lubec G (2008) Gel-based mass spectrometric analysis of recombinant GABA(A) receptor subunits representing strongly hydrophobic transmembrane proteins. J Proteome Res 7(8):3498–3506

Kantak KM (1988) Magnesium deficiency alters aggressive behavior and catecholamine function. Behav Neurosci 102(2):304–311

Kobayashi K, Haneda E, Higuchi M, Suhara T, Suzuki H (2012) Chronic fluoxetine selectively upregulates dopamine D(1)-like receptors in the hippocampus. Neuropsychopharmacology 37(6):1500–1508. doi:10.1038/npp.2011.335

Koenig JH, Ikeda K (1996) Synaptic vesicles have two distinct recycling pathways. J Cell Biol 135(3):797–808

Kreis P, Barnier JV (2009) PAK signalling in neuronal physiology. Cell Signal 21(3):384–393. doi:10.1016/j.cellsig.2008.11.001

Layer RT, Popik P, Olds T, Skolnick P (1995) Antidepressant-like actions of the polyamine site NMDA antagonist, eliprodil (SL-82.0715). Pharmacol Biochem Behav 52(3):621–627 (pii:0091-3057(95)00155-P)

Leonard AS, Bayer KU, Merrill MA, Lim IA, Shea MA, Schulman H, Hell JW (2002) Regulation of calcium/calmodulin-dependent protein kinase II docking to *N*-methyl-D-aspartate receptors by calcium/calmodulin and alpha-actinin. J Biol Chem 277(50):48441–48448. doi:10.1074/jbc.M205164200

Maj J, Rogoz Z, Skuza G, Sowinska H (1992) The effect of CGP 37849 and CGP 39551, competitive NMDA receptor antagonists, in the forced swimming test. Pol J Pharmacol Pharm 44(4):337–346

Merrill MA, Chen Y, Strack S, Hell JW (2005) Activity-driven postsynaptic translocation of CaMKII. Trends Pharmacol Sci 26(12):645–653. doi:10.1016/j.tips.2005.10.003

Murck H (2002) Magnesium and affective disorders. Nutritional Neurosci 5(6):375–389

Murck H (2013) Ketamine, magnesium and major depression—from pharmacology to pathophysiology and back. J Psychiatr Res 47(7):955–965. doi:10.1016/j.jpsychires.2013.02.015

Muroyama A, Inaka M, Matsushima H, Sugino H, Marunaka Y, Mitsumoto Y (2009) Enhanced susceptibility to MPTP neurotoxicity in magnesium-deficient C57BL/6N mice. Neurosci Res 63(1):72–75

Olsen JV, de Godoy LM, Li G, Macek B, Mortensen P, Pesch R, Makarov A, Lange O, Horning S, Mann M (2005) Parts per million mass accuracy on an Orbitrap mass spectrometer via lock mass injection into a C-trap. Mol Cell Proteomics 4(12):2010–2021

Plaznik A, Palejko W, Nazar M, Jessa M (1994) Effects of antagonists at the NMDA receptor complex in two models of anxiety. Eur Neuropsychopharmacol 4(4):503–512

Przegalinski E, Tatarczynska E, Deren-Wesolek A, Chojnacka-Wojcik E (1997) Antidepressant-like effects of a partial agonist at strychnine-insensitive glycine receptors and a competitive NMDA receptor antagonist. Neuropharmacology 36(1):31–37. pii:S0028390896001578

Ramboz S, Oosting R, Amara DA, Kung HF, Blier P, Mendelsohn M, Mann JJ, Brunner D, Hen R (1998) Serotonin receptor 1A knockout: an animal model of anxiety-related disorder. Proc Natl Acad Sci USA 95(24):14476–14481

Richardson-Jones JW, Craige CP, Nguyen TH, Kung HF, Gardier AM, Dranovsky A, David DJ, Guiard BP, Beck SG, Hen R, Leonardo ED (2011) Serotonin-1A autoreceptors are necessary and sufficient for the normal formation of circuits underlying innate anxiety. J Neurosci 31(16):6008–6018. doi:10.1523/JNEUROSCI.5836

Saatman KE, Bareyre FM, Grady MS, McIntosh TK (2001) Acute cytoskeletal alterations and cell death induced by experimental brain injury are attenuated by magnesium treatment and exacerbated by magnesium deficiency. J Neuropathol Exp Neurol 60(2):183–194

Sartori SB, Whittle N, Hetzenauer A, Singewald N (2012) Magnesium deficiency induces anxiety and HPA axis dysregulation: modulation by therapeutic drug treatment. Neuropharmacology 62(1):304–312

Singewald N, Sinner C, Hetzenauer A, Sartori SB, Murck H (2004) Magnesium-deficient diet alters depression- and anxiety-related behavior in mice—influence of desipramine and Hypericum perforatum extract. Neuropharmacology 47(8):1189–1197

Sowa-Kucma M, Szewczyk B, Sadlik K, Piekoszewski W, Trela F, Opoka W, Poleszak E, Pilc A, Nowak G (2013) Zinc, magnesium and NMDA receptor alterations in the hippocampus of suicide victims. J Affect Disord 151(3):924–931. doi:10.1016/j.jad.2013.08.009

Spasov AA, Iezhitsa IN, Kharitonova MV, Kravchenko MS (2008) Depression-like and anxiety-related behaviour of rats fed with magnesium-deficient diet. Zh Vyssh Nerv Deiat Im I P Pavlova 58(4):476–485

Tan SE, Wenthold RJ, Soderling TR (1994) Phosphorylation of AMPA-type glutamate receptors by calcium/calmodulin-dependent protein kinase II and protein kinase C in cultured hippocampal neurons. J Neurosci 14(3 Pt 1):1123–1129

Tang TT, Badger JD 2nd, Roche PA, Roche KW (2010) Novel approach to probe subunit-specific contributions to *N*-methyl-D-aspartate (NMDA) receptor trafficking reveals a dominant role for NR2B in receptor recycling. J Biol Chem 285(27):20975–20981. doi:10.1074/jbc.M110.102210

Trifilieff P, Rives ML, Urizar E, Piskorowski RA, Vishwasrao HD, Castrillon J, Schmauss C, Slattman M, Gullberg M, Javitch JA (2011) Detection of antigen interactions ex vivo by proximity ligation assay: endogenous dopamine D2-adenosine A2A receptor complexes in the striatum. Biotechniques 51(2):111–118. doi:10.2144/000113719

Trullas R, Skolnick P (1990) Functional antagonists at the NMDA receptor complex exhibit antidepressant actions. Eur J Pharmacol 185(1):1–10. doi:10.1016/0014-2999(90)90204-J

Weinhofer I, Forss-Petter S, Zigman M, Berger J (2002) Cholesterol regulates ABCD2 expression: implications for the therapy of X-linked adrenoleukodystrophy. Hum Mol Genet 11(22): 2701–2708

Wenthold RJ, Petralia RS, Blahos J II, Niedzielski AS (1996) Evidence for multiple AMPA receptor complexes in hippocampal CA1/CA2 neurons. J Neurosci 16(6):1982–1989

Whittle N, Li L, Chen WQ, Yang JW, Sartori SB, Lubec G, Singewald N (2011) Changes in brain protein expression are linked to magnesium restriction-induced depression-like behavior. Amino Acids 40(4):1231–1248

Wlaz P, Kasperek R, Wlaz A, Szumilo M, Wrobel A, Nowak G, Poleszak E (2011) NMDA and AMPA receptors are involved in the antidepressant-like activity of tianeptine in the forced swim test in mice. Pharmacol Rep 63(6):1526–1532

Yakel JL, Vissavajjhala P, Derkach VA, Brickey DA, Soderling TR (1995) Identification of a Ca^{2+}/calmodulin-dependent protein kinase II regulatory phosphorylation site in non-*N*-methyl-D-aspartate glutamate receptors. Proc Natl Acad Sci USA 92(5):1376–1380

Zukin RS, Bennett MV (1995) Alternatively spliced isoforms of the NMDARI receptor subunit. Trends Neurosci 18(7):306–313. doi:10.1016/0166-2236(95)93920-S